Engineering *Toxoplasma* transgenic tissue cysts.

David D. Hong[1], Krista Brooks[1], Amber L. Goerner[1], Edward A. Vizcarra[2], Luiza N. Loges[1], Emma H. Wilson[2], and Michael W. White[1&]

[1]Department of Internal Medicine, Division of Infectious Disease and International Medicine, Morsani College of Medicine, University of South Florida, Tampa, Florida, USA. [2]Division of Biomedical Sciences, School of Medicine, University of California, Riverside, Riverside, California, USA

Running title: *Toxoplasma* cyst genetics

Key Terms: Apicomplexa, *Toxoplasma gondii*, development, tissue cyst, latency, chronic toxoplasmosis

[&]Address correspondence to:

Michael W. White
Department of Internal Medicine
Division of Infectious Disease and International Medicine
University of South Florida
3720 Spectrum Blvd, Suite 304
Tampa, FL 33612
email: mwhite.usf@gmail.com
office 813-974-8411
Fax 813-974-0804

Abstract

Current approaches to find therapeutic solutions to treat and prevent reactivation of toxoplasmosis have suffered from limited accessibility to the relevant *Toxoplasma* stages and a lack of accurate in vitro developmental models. The loss of developmental competency in vitro that is exacerbated during the generation of transgenic tachyzoites is also a major impediment to understanding the molecular basis of bradyzoite recrudescence, which is the central feature of reactivation. We have developed an innovative ex vivo model of bradyzoite recrudescence and applied this method to successfully modify *Toxoplasma* genes while avoiding the problems caused by continuous in vitro cell culture. We present four protocols required to engineer in vivo transgenic tissue cysts: **1)** the reliable production of in vivo tissue cysts and excysted bradyzoites, **2)** the use of fast-growing parasites from ex vivo bradyzoite infections to successfully generate transgenic tissue cysts in mice, **3)** the cloning of transgenic bradyzoites via single cyst infections, and finally, **4)** the long term cold storage and recovery of transgenic tissue cysts in brain tissue homogenates. We demonstrated these protocols by knocking out the *Toxoplasma* HXGPRT gene and the gene encoding the ApiAP2 transcription factor, AP2IX-9 in tissue cysts from mice. Unexpectedly, the knockout of the AP2IX-9 gene in the Type II ME49EW strain eliminated one of the three developmental pathways initiated by the bradyzoite; host-dependent bradyzoite to bradyzoite replication.

Introduction

Toxoplasma gondii infections continue to be a public health hazard for millions of individuals that are exposed to this pathogen annually. More than 50 million individuals in the US are chronically infected with *Toxoplasma gondii* and thousands of healthy individuals develop eye disease due to this infection that can lead to permanent vision loss. The Centers for Disease Control and Prevention considers *Toxoplasma* one of the five most important neglected parasitic infections. Individuals can be treated (despite significant side effects) for acute clinical toxoplasmosis, however, no current drug successfully treats or prevents the tissue cyst that is responsible for long-term infections. This therapy failure leaves infected individuals vulnerable to disease relapse throughout their lifetimes.

Toxoplasma infections are life-long due to the development of the bradyzoite tissue cyst, which is effectively invisible to the immune system [1]. Despite the important clinical consequences of this developmental pathway, the molecular basis of the switch mechanisms that control formation and

recrudescence of the tissue cyst are still poorly understood. Current in vitro models based on pH8.2-media induction have been useful in defining the early events of tachyzoite to bradyzoite switching, however, it is well understood these models do not fully reproduce in vivo tissue cyst development or recrudescence. In our own labs, contradictory results from in vitro model versus in vivo animal experiments has limited developmental studies. The lack of an accurate model of bradyzoite developmental biology is hindering advances in understanding the parasite mechanisms that cause chronic toxoplasmosis.

The genetic tool kit for *Toxoplasma* is one of the best in eukaryotic cell research. *Toxoplasma* genetic methods have been used to understand the molecular basis of the peculiar tachyzoite cell cycle, to learn how tachyzoites invade and establish intracellular life, and to discover the mechanisms governing parasite-host cell interaction. Unfortunately, current genetic methods were designed for the tachyzoite stage and are less successful for studying stages responsible for chronic disease and disease recrudescence due to the unique biology of the bradyzoite stage. In this paper we introduce protocols that overcome the barriers to applying genetic methods to in vivo bradyzoites. We demonstrate methods to scale the production of tissue cysts from animals and introduce new genetic approaches that use ex vivo bradyzoites to engineer in vivo transgenic tissue cysts.

Results

Maintenance and scale production of developmentally competent tissue cysts.

The ME49 strain used in these studies (designated ME49EW) has been exclusively maintained for >20 years in vivo by alternating passage through resistant and sensitive mouse strains in order to sustain efficient tissue cyst production (Fig. 1). The two mouse strains used in these studies, are the disease sensitive CBA/j strain and relatively disease resistant Swiss Webster (SWR/j) strain. From an infection of 10 cysts, the ME49EW strain consistently produced thousands of tissue cysts in CBA/j mice at 40 day post-infection (d.p.i.) and a lower, but still robust cyst numbers in SWR/j mice (Fig. 1A). Alternating passage between CBA/j and SWR/j mouse strains was required to maintain robust tissue cyst numbers in mouse brain tissue (Fig. 1B). Repeated passage in CBA/j mice led to a progressive reduction in brain tissue cyst number that could be restored by a single passage through SWR/j mice (Fig. 1B, 30 d.p.i. cyst counts). The molecular basis of restoring declining tissue cyst numbers by passage in SWR/j mice is under investigation in our laboratories.

In the current studies, SWR/j mice were used for maintenance purposes (30-60 d.p.i.), while CBA/j mice were used for scaled tissue cyst production (30-45 days d.p.i.). In CBA/j mice, ME49EW cyst numbers increased between 30 and 50 d.p.i. A 10 cyst infection i.p. yields ~2,500 cysts/brain at 30 days with an average 50% increase in cyst numbers >40 d.p.i. [2]. For production purposes, a 10% mortality by 40 days post-infection was factored for ME49EW strain infections of CBA/j mice. Tissue cyst numbers can vary considerably, with 40 d.p.i. yielding 1,500-10,000 cysts per mouse. Doses higher than 10 cysts can be used, however, increases in cyst yields per mouse were offset by higher CBA/j mortality.

In the absence of a suitable laboratory model to investigate native bradyzoite biology, we optimized ME49EW tissue cyst and bradyzoite purification protocols to reliably yield an average of 1.4 million purified bradyzoites per CBA/j mouse (Fig. 2 and Protocol S1). The ME49EW/CBA/j model for the production of tissue cysts has been run at increased scale (25-50 mice/month) in our laboratories for several years and the consistency of this model for obtaining native bradyzoites is shown in the Figure 2 production data. Two key changes were introduced to the cyst isolation protocol that improved the consistency and yields of tissue cyst purifications (see Protocol S1). **1.)** Only the mouse cortex was harvested for tissue cyst processing. Anatomical mapping of mouse brain infections [3] recently determined the majority of tissue cysts are localized to the brain cortex and not in the cerebellum. In our protocols, removing the white fibrous cerebellum improved homogenization of brain tissue without significant loss of cysts (<10% losses). **2.)** Whole brain cortices were kept cold (0-4°C) in 1xPBS from the time of harvest until tissue homogenization the next morning. Cold incubation of mouse brain tissue improves homogenization and cyst yields with no discernable effect on tissue cyst viability or the ability of excysted bradyzoites to invade host cells and initiate recrudescence [2]. Homogenates of freshly harvested brain tissue suffered cyst losses (30-50% loss) during percoll gradient purification due to cyst trapping in incompletely homogenized tissue.

Establishing ex vivo cell culture models.

In order to establish an ex vivo model of bradyzoite recrudescence for the purpose of developing new genetic strategies, we investigated the use of primary mouse neonatal astrocytes, which are relatively easy to culture and are a major host cell that bradyzoites encounter during recrudescence in brain and eye tissue [4-6]. Initial ME49EW bradyzoite infections of HFF cells yielded poor medium-term ME49EW parasite growth, and were

therefore, not used for developing new genetic protocols. We first evaluated ME49EW bradyzoite-initiated growth in astrocyte specialized media at two oxygen gas conditions (5% versus 21%). We reasoned oxygen conditions might influence ex vivo bradyzoite models due to the hypoxic oxygen environment of brain tissue where in vivo ME49EW tissue cysts reside [7]. Short term parasite growth (Day 1-3) in bradyzoite-infected astrocytes was not affected by oxygen levels, however, in astrocyte cultures beyond Day-3, parasite growth was negatively affected by atmospheric oxygen levels (21%)(Fig. 3A). A similar oxygen effect on ME49EW bradyzoite recrudescence was also observed in HFF cells [2]. As a consequence of these experiments, lower oxygen conditions (5%) in hypoxic chambers were used to cultivate ME49EW parasites throughout these studies. To avoid host cells becoming a limiting factor, and to allow for continuous tracking of the growth rate, parasites were passed after Day 3 and Day 5 (and sometimes after Day 7) post-bradyzoite infection. Similar to HFF cells, recrudescing populations progressed through two growth phases in primary astrocytes [2]. Parasites through Day-5 post-bradyzoite infection grew relatively fast compared to parasites beyond Day-5 and especially beyond Day-7 (Fig. 3B). Thus, to avoid the slow-growing phase of recrudescence, parasites needed to be cultured for 7 days or less post-bradyzoite infection in primary astrocytes.

Because of a focus on the fast-growing phase of bradyzoite recrudescence for developing new genetic models, we assessed the extracellular viability of rapidly growing Day 2-populations in HFF cells or astrocytes. Day-2 parasites were purified from bradyzoite-infected cultures and then resuspended in culture media. Extracellular parasites were sampled every 6 h over a 30 h period and inoculated into either HFF or astrocyte monolayers. Plaque formation was quantified 48 h later by IFA assay. Fast-growing ME49EW Day 2-parasites from either host cell type were much less stable extracellular (Fig. 3C) with ~88% of the parasites dying by 6 h in media (2-3 h half-life). By contrast, the lab-adapted RH strain parasites were more stable; extracellular incubation for 24 h in media was required before ~90% of RH parasites died. We examined whether extracellular sensitivity was a characteristic of native strains (i.e. less cell culture adapted) by examining the stability of early passage Type I strain, GT1, which was used to produce genetic crosses in cats [8]. Similar to ME49EW Day-2 parasites, GT1 tachyzoites were more sensitive to incubation outside the host cell with ~95% of parasites lost by 12 h extracellular (Fig. 3C). Taken together, these results demonstrate that working with native strains requires careful handling with time outside the host cell minimized.

Finally, it was important to evaluate whether cultivation of native ME49EW parasites in astrocytes would affect the capacity to form tissue cysts in mice. Day 30 brain tissue cyst counts of CBA/j mice infected (10,000 parasites/mouse i.p) with parasites harvested at Day-3, -7 and -14 post-bradyzoite infection were compared to cyst numbers obtained in excysted bradyzoite infections. We previously determined that tissue cyst numbers were similar in mice infected with excysted bradyzoites or Day-3 parasites (see ref. [2]). By contrast, cyst counts dropped significantly in CBA/j mice infected with Day 7 or Day 14 parasites (Fig. 3D). The results were presented here as a percentage of the cyst yields produced by excysted bradyzoite infections. A second round of infection using 10 tissue cysts i.p. (standard dose) obtained from the first-round mice demonstrated a permanent loss of cyst forming capacity had occurred in parasites cultivated for 14 days but not for 7 days in primary astrocytes (Fig. 3D). Like the restricted period of ME49EW parasite fast-growth, these results defined an important time constraint for how long ME49EW parasites can be grown in vitro (one week) before cyst numbers permanently decline.

Engineering of transgenic tissue cysts.

Current genetic protocols rely on highly modified tachyzoite strains (e.g. Δhxgprt, Δku80, TIR1- and GFP-expression) that were well adapted to grow in HFF cells, and as a consequence poorly form tissue cysts in mice when compared to native strains like ME49EW [2]. Our goal was to improve genetic methods by eliminating the parent strain development competency problem and reduce in vitro passage. A sobering reality for new genetic method development was the surprisingly short timeframe before passages in astrocyte cell culture (3-4 passages) permanently caused reductions of tissue cysts numbers in mice (Fig. 3D). Working within a 7 day astrocyte culture restriction, we have developed a successful approach for genetically modifying *Toxoplasma*, while preserving developmental competency (see Fig. 4, graphic overview). The new method was developed and tested using a plasmid design that targeted the HXGPRT gene for replacement with a DNA insert containing the pyrimethamine-resistant TgDHFR selectable marker [9] and GFP and firefly luciferase reporters (see Fig. 4 cartoon). The key to a development-sparing genetic model was the fast-replicating tachyzoite stage that forms early in ME49EW ex vivo bradyzoite recrudescence [2]. The rapid growth of these parasites provides a ~5-fold parasite amplification by Day 2 (Fig. 3A) that together with the reduced number of parasites needed ($1x10^7$) for nucleofection necessitated fewer infected mice in these protocols (5-8 mice per nucleofection). Robust growth of Day-2 ME49EW parasites was the key ingredient

for comparatively high transformation frequency equal to or exceeding the Type I RH tachyzoite that were both ~10-fold higher than HFF-adapted ME49B7 tachyzoites (Fig. 4, GFP+ frequency in FACS plots). Conventional plaque assays to measure transformation was not possible in the bradyzoite ex vivo recrudescence model, and thus, transformants were estimated by flow cytometric quantification of bright GFP+ parasites (>10^3 FL 1 fluorescence) following four days of selection in 0.5 μM pyrimethamine (Day 3 through Day 6 post-bradyzoite infection). The GFP+-recombinant to nonrecombinant ratios were 1/171 for Day-2 parasites, 1/223 for RH, and 1/1,653 for ME49B7.

To limit the cell culture of ME49EW recrudescing parasites, GFP+ transformants were FACS sorted at Day-7 post-bradyzoite infection (3 days of pyrimethamine selection) and >50,000 GFP+ parasites were collected. We reanalyzed 500 parasites by flow cytometry and confirmed a >150 fold GFP+ enrichment over pre-sorted populations (88% GFP+, Fig. 5A). A group of five CBA/j mice were infected using a dose of 10,000 GFP+ parasites i.p. per mouse. At 30 d.p.i., the mice were euthanized and total cyst counts and percent GFP determined in brain cortices. All mice were infected with >1,600 brain tissue cysts and the GFP+ tissue cyst positivity varied from 52% to 72%. Tissue cysts were either 100% GFP+ or 100% GFP-, no mixed tissue cysts were observed. The next step in the goal to produce transgenic tissue cysts was to obtain clonal GFP+ cyst isolates.

Cloning and preserving ME49EW transgenic tissue cysts.

The most common protocol for cloning transgenic tachyzoites utilizes limiting dilution of parasites in 96 well plates. Unfortunately, this approach was not suitable given the requirement to limit time in cell culture to one week. The tachyzoite parasitophorus vacuole is formed from a single parasite infection, and thus, harbors clonal intravacuole parasites. Tissue cysts are derived from individual PVs [10], and are therefore, also expected to be composed of clonal parasites. We investigated whether cloning transgenic isolates by single tissue cyst infections in mice was feasible. We first evaluated the reliability of very low dose ME49EW cyst infections by mixing GFP+ and GFP- cysts 1:1 and infecting CBA/j mice with 2 cysts i.p. At 30 d.p.i., tissue cyst numbers and the fraction of GFP+ versus GFP- tissue cysts were determined (Fig. 6A). There was a 1 in 4 theoretical chance that a 2 cyst infection of mice would be homogeneous GFP+ or GFP- (25% each), although in practice it was unlikely all mice would receive a precise two cyst infection. All 20 mice were successfully infected (one mouse died from the *Toxoplasma* infection before 30 d.p.i.) with 5 mice infected

with only GFP+ cysts and 3 mice infected with only GFP- cysts. The remaining 11 mice were infected with various mixtures of GFP+ and GFP- cysts including ~1:3, ~1:4, ~1:5, and some ~1:20. Because we did not control for cyst size (i.e. variable bradyzoite numbers) these types of mixtures were expected. Importantly, there were no individual cysts with mixtures of GFP+/GFP- parasites in the hundreds of cysts we examined microscopically confirming the clonality of parasites within individual cysts.

The infection success with low cyst numbers led us to test methods to isolate single cysts in brain homogenates or from percoll-purified cysts. Limiting dilution of cysts in 96 well optical plates (1 cyst/100μl) followed by microscopic screening was an effective strategy to isolate single cysts (see Protocol S3 for details). The contents of wells with single cysts were loaded into syringes and used to infect CBA/j mice (percoll or homogenate diluted preparations). All mice were successfully infected and yielded hundreds to thousands of clonal tissue cysts in brain tissue at 30 d.p.i. (Fig. 6B). The 100% GFP+ phenotype of these clones were stable through several rounds of CBA/j or SWR/j infections.

With a suitable protocol developed, we cloned HXGPRT knockout parasites using the cysts from a second nucleofection that was followed by a GFP+ FACS sort and CBA/j infection (at 30 d.p.i., 4 mice were 100% GFP+ and one mouse was 33% GFP+). GFP+ tissue cysts in brain homogenate from one of the mice was diluted to 1 cyst/100 μl and plated into 96 well optical plates. Eight single GFP+ cysts were identified and used to infect CBA/j mice (i.p.). At 30 d.p.i., brain cortex tissue was harvested and cyst counts and GFP expression determined. One mouse had no cysts, while another only had GFP- cysts. The remain six mice had cyst numbers ranging from 100 to 8,000 cysts per brain cortex. We selected four homogenates to move forward to PCR screens; Brain #1-600 cysts, Brain #2-1,600 cysts, Brain #3-700 cysts, and Brain #6-8,000 cysts. The brain homogenates were diluted to 1 cyst/100 μl with PBS and plated in 96 well optical plates. Selected wells containing 1-3 cysts were processed for DNA using Protocol S3 and analyzed using the PCR strategy in Figure 6C. All DNA templates produced the right and left arm DNA fragments indicating a successful HXGPRT gene knockout. Homogenates #1, #2, and #8 cysts did not amplify an internal DNA fragment from the native HXGPRT gene indicating they were clean HXGPRT knockouts, while brain #3 DNA template did amplify the internal fragment indicating this mouse was likely dually infected with the HXGPRT

knockout and ME49EW parent parasites. Homogenates from mouse brain #1, #2, and #8 were frozen at -80°C using Protocol S4.

Engineering an AP2IX-9 gene knockout in ME49EW tissue cysts.

A major class of transcription factors in *Toxoplasma* are nuclear proteins distantly related to the APETLA family of transcription factors of plants [11]. The *Toxoplasma* genome encodes >60 of these factors, one of the largest collection of ApiAP2 genes in the Apicomplexa family of parasites. A subset of ApiAP2 factors are developmentally expressed and have functions in regulating *Toxoplasma* life cycles [12-14]. Recently, we determined that AP2IX-9 was the highest expressed ApiAP2 mRNA in mature in vivo ME49EW bradyzoites [2]. This result was unexpected as previous studies only detected transient expression of AP2IX-9 mRNA when tachyzoites were induced to differentiate in vitro to bradyzoites under alkaline-media conditions [12, 13]. Because of this discrepancy, we re-examined the function of AP2IX-9 using our new genetic methods. Utilizing the strategy used to knockout the HXGPRT gene (Fig. 4A), the AP2IX-9 gene was deleted in ME49EW Day-2 parasites by nucleofection, which was followed by 3 day pyrimethamine selection, FACS sorting of GFP+ parasites and CBA/j i.p. infections. At 30 d.p.i., we isolated single GFP+ tissue cysts and infected CBA/j mice. We verified the AP2IX-9 knockout in this clonal round of infection using the PCR strategy outlined in Figure 7A. PCR analysis confirmed a successful knockout of AP2IX-9 in GFP+-clone 9 and confirmed the absence of AP2IX-9 mRNA in clone 9 parasites (Fig. 7A). The ME49EW::Δ*ap2IX-9* clone was then used to quantify tissue cyst formation in CBA/j mice. Groups of CBA/j mice were infected with ME49EW::Δ*ap2IX-9* or ME49EW parent strain tissue cysts (10 cysts i.p./mouse) and brain tissue cyst numbers quantified at 30 d.p.i. Knockout of AP2IX-9 in the ME49EW strain did not prevent or significantly diminish tissue cyst formation in CBA/j brain tissue (Fig. 7B).

We next purified ME49EW::Δ*ap2IX-9* bradyzoites to further study the role of AP2IX-9 in ME49EW bradyzoite recrudescence. Primary mouse astrocytes were infected with ME49EW::Δ*ap2IX-9* or ME49EW parent bradyzoites from in vivo cysts followed by the analysis of growth and development over 7-14 days. The parasite growth changes from fast to slow growth previously described during ME49EW bradyzoite recrudescence [2] were detected in astrocytes or HFF cells infected with either ME49EW::Δ*ap2IX-9* or ME49EW parent bradyzoites (Fig. 7C). Recent experiments demonstrated that infections with ME49EW

parent bradyzoites led to bradyzoite differentiation into the tachyzoite stage as well as extensive replication of ME49EW bradyzoites (SRS9+ only) in astrocytes but not HFF cells [2]. Strikingly, bradyzoite to bradyzoite replication of the ME49EW parent was absent in ME49EW::Δ*ap2IX-9* recrudescing populations regardless of the host cell type infected (astrocyte only results shown Fig. 7D). A small number of SRS9+ only vacuoles were detected during the first three days of bradyzoite recrudescence in astrocytes with the invading bradyzoite the majority of these vacuoles in Day-1 infected host cells. The replication that was observed for the very few bradyzoite vacuoles (SRS9+ only) detected in Day -2 and -3 of recrudescence was restricted to 1-2 divisions (Fig. 7E). Only in SRS9+/SAG1+ and SAG1+ vacuoles did we observe robust ME49EW::Δ*ap2IX-9* parasite replication (Fig. 7C). These results confirmed that only bradyzoite-to-tachyzoite development was active in ME49EW::Δ*ap2IX-9* infected astrocytes.

Discussion

There have been steady advances in genetic methods for *Toxoplasma* since the first transient and stable transfection of tachyzoites nearly 30 years ago [15, 16]. An expanded list of positive and negative selectable markers now includes seven drug/gene pairs providing positive and/or negative genetic selection (DHFR/pyrimethamine, CAT/chloramphenicol, HXGPRT/mycophenolic acid, BLE/phleomycin, UPRT/fluorodeoxyuridine, HSTK/gancyclovir, AA transport/Sinefungin [9, 15, 17-19]. Gene replacement and DNA transformation frequencies have been improved by eliminating nonhomologous DNA repair [20, 21] and targeting specific chromosome breaks in or near target genes [22]. Because genetic deletion is unsuitable for required and essential genes, conditional knockdown methods have been developed that operate transcriptionally or post-translationally [23, 24]. The high frequency of recombination achievable in laboratory strains like the Type I RH strain has permitted multiple forward genetic experiments with whole-genome CRISPR identification of required tachyzoite growth genes a recent example [25-27]. In this study, we have taken advantage of the extensive *Toxoplasma* genetic “tool kit” to successfully produce transgenic tissue cysts in mice.

Nearly all methods to genetically modify *Toxoplasma* developed over the last 30 years employed a tachyzoite strain that was well adapted to grow in HFF cells. Regrettably, this was not a good strategy for studying the biology of parasite stages other than the tachyzoite. It is well known that repeated passage in

HFF cells exacerbates the loss of developmental competency (reviewed in refs. [28, 29]). When *Toxoplasma* is adapted to HFF cells, a number of interrelated characteristics change including increases in growth rates, extracellular viability and mouse virulence, while in vivo development dramatically decreases. Our results here demonstrate that the loss of *Toxoplasma* developmental competency occurs earlier in cell culture than most appreciate. Working with the unadapted-Type II strain ME49EW, we demonstrated that in as little as two weeks in cell culture ME49EW tachyzoites show permanent losses in tissue cyst formation in mice. Repeated passage in a single mouse strain can also cause diminished tissue cyst development (Fig. 1B), which can be ameliorated by strictly adhering to a protocol of alternating tissue cyst infections between sensitive and resistant mouse strains. Unfortunately, there is no easy method we have discovered to reverse reduced tissue cyst formation once the loss is permanent.

To achieve efficient genetic transformation while preserving developmental competency, we introduced a number of key innovations into the current *Toxoplasma* genetic methodology. The deep dormancy of native mature bradyzoites [2] is an important factor in the tolerance of these parasites to extended cold incubation, which improves cyst purification, and to the brief harsh acid-protease conditions that disrupt the tissue cyst wall during excystation to purify free bradyzoites. Developmental competence is affected by the type of host cell used [2], therefore, we replaced the standard HFF host cell with primary mouse astrocytes. Other cell types may be suitable, although the ease of culturing primary astrocytes makes this host cell a good choice. Developmentally competent parasites in astrocytes were heathier when cultured under 5% oxygen rather than standard atmospheric oxygen conditions, which can be achieved with inexpensive hypoxic chambers commonly used to culture *Plasmodium falciparum* merozoites in vitro. All genetic experiments were initiated with ex vivo ME49EW bradyzoite infections of astrocytes, which provides a uniform experimental starting point and eliminates the creeping in vitro adaption of low passage strains. Our results over three years of testing demonstrate that bradyzoite yields from ME49EW mouse infections are stable and readily scalable to support multiple genetic experiments. Critically, high transformation efficiency requires a parasite undergoing active chromosome replication, which is challenging when trying to transfect low passage, slow-growing tachyzoites that were recently adapted to HFF cell culture (in the hope that developmental competence will be preserved). Our new genetic models based on ME49EW bradyzoite recrudescence [2] eliminates these issues. Ex vivo ME49EW bradyzoites convert to fast-growing

developmentally competent tachyzoites in astrocytes that transform at frequencies often exceeding the best RH strain transformation rates. It is intriguing that previous studies of these novel fast-growing tachyzoites, which also form in sporozoite infections [30], determined their transcriptome was more closely related to the RH strain than other lab strains [31]. The best method for introducing plasmid DNAs into fast-growing ME49EW tachyzoites was via nucleofection using CRISPR designs. Finally, we combined a short drug selection in astrocytes with GFP-FACS sorting in order to return highly enriched transgenic parasites (~150 fold enriched) to mice within 7 days of the initial bradyzoite infection. We believe this timeframe provides for adequate dissemination and new tissue cyst seeding in mouse brain that we determined was complete by 12 days post-bradyzoite infection of mice [2]. Other procedures developed were equally essential for successful genetic modification of tissue cysts. The effectiveness of single tissue cyst cloning and mouse infection was demonstrated and the ability to freeze tissue cysts in brain tissue homogenates for later infections was also important. We anticipate other improvements to follow including positive selection of transgenic parasites in mice and genetic knock-in strategies to permit epitope tagging and the application of auxin-based conditional knockout strategies. We are currently evaluating a new one step protocol for utilizing auxin-based approaches and we are testing alternate gene replacement protocols that will permit genetic complementation in transgenic tissue cysts.

Our studies of the transcription factor AP2IX-9 in HFF in vitro models [13] determined that overexpression of AP2IX-9 repressed the alkaline-stress induction of some bradyzoite gene expression, and also inhibited alkaline-stress induced cyst wall formation [13]. From these results, we concluded AP2IX-9 must function to negatively regulate tachyzoite to bradyzoite development, although at the time we were unable to verify this mechanism in a competent in vivo model of *Toxoplasma* development. Later studies determined that deletion of the AP2IX-9 gene did not inhibit DBA+-cyst wall formation in vitro, while it modestly enhanced cyst wall formation [12]. Targeted CRISPR screens of DNA binding proteins, also determined that AP2IX-9 was not essential for tissue cyst formation in vitro [32]. It was therefore, not surprising that the deletion of the AP2IX-9 gene in the developmentally competent ME49EW strain did not prevent in vivo tissue cyst formation (tachyzoite to bradyzoite) in murine brain. This left us with the question of why AP2IX-9 is the highest expressed ApiAP2 mRNA in mature tissue cysts [2]. The bradyzoite is the pluripotent stage of the *Toxoplasma* life cycle. Bradyzoite-to-tachyzoite, bradyzoite-to-bradyzoite, and bradyzoite-to-merozoite are

pathways initiated by bradyzoite infections. It is clear some of these pathways are host-dependent while others are not [2]. While deletion of AP2IX-9 in ME49EW tissue cysts did not block bradyzoite-to-tachyzoite recrudescence in astrocytes, it completely eliminated the pathway of bradyzoite-to-bradyzoite replication that is active in ME49EW parent infections of astrocytes but not fibroblasts [2]. The function of bradyzoite replication is not understood. This developmental process may be required for long term maintenance of the tissue cysts in animals or it may prepare the bradyzoite for transmission to different animal hosts, which were functions not evaluated here. The role of AP2IX-9 in bradyzoite-to-merozoite was also not investigated. Further studies will be needed to fully understand the role of AP2IX-9 in bradyzoite developmental biology. The developmentally competent transgenic cysts lacking AP2IX-9 generated in this study now make these studies possible.

In summary, we have developed ex vivo bradyzoite protocols that were combined with the current *Toxoplasma* genetic "tool kit" to enable for the first time the generation of transgenic tissue cysts in mice. The critical parasites of this new genetic model are the unadapted ME49EW strain from which developmentally competent bradyzoites from in vivo tissue cysts can be purified and via ex vivo bradyzoite infections the unique fast-growing tachyzoite capable of efficient transformation can be produced. We have used these new protocols to revisit the AP2IX-9 mechanism [13] that we likely got wrong using in vitro models of bradyzoite development, while at the same time discovering a potential new developmental ApiAP2 mechanism that was inaccessible to these conventional in vitro models. The loss of developmental competency in vitro that is exacerbated in current protocols producing transgenic strains is a major impediment to understanding the molecular basis of bradyzoite pluripotency. We believe the new genetic methods presented here can overcome these problems. As we add new features to the ex vivo genetic protocols, such as gene conversion to auxin control in tissue cysts, we will repost this preprint with the new protocols.

Material and Methods

Parasite strains and host cells.

The Type II ME49EW strain was kindly provided by Emma Wilson (U. California Riverside). The strain ME49EW1 was obtained by forced adaptation of the parent ME49EW strain to grow well in human foreskin fibroblasts (HFF) under standard culture conditions used to grow HFF-adapted strains and then cloned by

limiting dilution. ME49EW1 was used here to evaluate paarasite stability outside the host cell (Fig. 3C). HFF-adapted laboratory strains used in this study were RH (Type I RH Δ*hxgprt*)[33] and GT1 (low passage Type 1 strain)[34]. Mouse primary astrocytes were purchased from ScienCell (#M1800) and cultured using media and methods provided by ScienCell. Confluent HFF or primary astrocyte monolayers were inoculated at various times with excysted bradyzoites, lab strains or recrudescing populations at a MOI ~0.5.

Animal experiments.

All animal research was conducted in accordance to the Animal Welfare Act. CBA/J, and SWR/J #689 mice obtained from Jackson Laboratory (Jackson ImmunoResearch Laboratories, Inc., West Grove, PA, USA) were maintained in a pathogen free vivarium under the Institutional Animal Care and Use Committee (IACUC) protocols established at the University of South Florida, Tampa. The ME49EW strain was sequentially passed through 5- to 6-week old female mice by first infecting resistant strain SWR/J (Swiss Webster) with 10 cysts in 200μl of cortex homogenate by intraperitoneal (i.p.) injection. Tissue cysts in brain homogenates from infected SWR/J mice were then used to infect CBA/J, sensitive mice (10 cysts in 200μl diluted brain homogenates, i.p.). This alternating passage was strictly followed in all experiments.

Brain homogenate preparation. At 30-60 days PI, infected SWR/J or CBA/J mice were euthanized, brain cortices dissected and placed in 3ml of cold PBS (cerebellum was discarded as it contained <10% of total brain tissue cysts). Tissue homogenization and tissue cyst yields were significantly improved (tissue cyst numbers >50% higher) by storing infected brain cortices overnight at 4°C in PBS. In direct comparisons, we determined tissue cysts held in brain tissues for up to 24 h in cold PBS were viable, fully infectious, and yielded active excysted bradyzoites. After the 4°C overnight storage in 3 ml of 1xPBS, cortices were more easily serially homogenized through 18, 20 and finally, 22 gauge sterile needles. Tissue cyst quality and enumeration was determined by a full examination of 30μl (x 3) of homogenate spread on a microscope slide. All tissue cyst mouse inocula used in this study were diluted to 10 cysts in 200μl in 1xPBS. In addition, the quantification of brain tissue cyst counts in mice infected with various parasite sources followed these protocols and were determined in triplicate. For full details of brain cortex harvest and cyst and bradyzoite isolation see supplement Protocol S1.

Infections of mice with laboratory strains and recrudescing populations. ME49EW bradyzoites and parasites at various times during recrudescence in HFF or astrocyte cells were purified from host cell monolayers by standard scrape, needle pass, and filter methods and diluted to the appropriate parasite concentration in PBS.

In vitro cell culture experiments.

Experimental details of the ex vivo bradyzoite recrudescence model can be obtained in Goerner et al. 2020 [2]. Native bradyzoites in mouse brain reside in a hypoxic tissue environment, and as a consequence ME49EW strain bradyzoite-infected host cells are healthier when cultured at 37°C under 5% oxygen in media containing 5% FBS. Growth media recipe for HFF cells (500ml): use power DMEM media with L-glutamine and sodium pyruvate (6.74g), add 12.5ml 1M HEPES buffer, 25ml FBS, and 5 ml of antibiotic mix (Pen-strep and amphotericin B). The media was then warmed to 37°C and adjusted to pH to 7.4 using 4M KOH. For astrocyte cultures, we used ScienCell media and supplements (e.g. 1% GlutaMAX supplement). To achieve hypoxia conditions, a hypoxia chamber charged with mixed gas (90% nitrogen/5% oxygen/5% CO_2) for 3 min and placed on the shelf of a CO_2 incubator at 37°C. See https://www.stemcell.com/hypoxia-incubator-chamber.html for the chambers used in these studies. All experiments in these studies were run under 5% oxygen conditions except for part of the population growth studies of Figure 3A.

Growth rate doublings. Post-excysted bradyzoites and recrudesing populations were inoculated onto 6 well coverslips of HFF or primary astrocyte cells and at various times were fixed and stained using an anti-toxoplasma antibody (abcam, ab138698). Vacuole sizes at each timepoint were determined by counting 50 random vacuoles in triplicate on a Zeiss Axiovert fluorescent microscope.

Visualization of parasite growth and development. ME49EW bradyzoites and various recrudescing populations were inoculated onto 6 well glass coverslips of HFF or astrocyte cells at 0.5 MOI. Infected coverslips were fixed with 4% PFA for 10min. Cells were permeabilized with either 100% acetone or 0.25% Triton-X for 10min. Cells were blocked with 1% BSA for 30min, followed by a 1 h incubation of the following primary antibodies diluted in blocking buffer: rabbit-anti SRS9 [1:1000] and mouse-anti SAG1 [1:1000](kindly provided by John Boothroyd, Stanford U.), rabbit-anti-Toxo [1:500] (Abcam). Secondary antibody master mix were incubated for 1 h: Goat-anti-rabbit-AF568 [1:1000], Goat-anti-mouse-AF488 [1:1000], DAPI (1mg/ml). All incubations were done at room temperature, and all washes used 1XPBS.

Extracellular viability. Day 2-recrudesing ME49EW parasites (bradyzoite infection of HFF or astrocytes) and lab-adapted strains, ME49EW1, RH and GT1 parasites were purified and resuspended in 37°C growth media (no host cells). The host-free parasites (10,000/cover slip) were used to immediately inoculate cover slips of the host cell type they were obtained from, and then again, at 6, 12, and 24 h (only 0, 6, and 12 h are shown). Parasites were incubated at 37°C throughout the experiment and ME49EW parasites were cultured in hypoxic chambers, while lab-adapted strains were cultured under standard ambient oxygen conditions. Infected coverslips were left to grow undisturbed for ~4 days prior to being fixed and IFA analysis performed using anti-toxo primary antibody. Microscopic quantification of parasite plaques was determined by counting the number of vacuoles per field for a total of 10 fields (in triplicate). Percent survival was determined in comparison to the time zero infections.

HXGPRT and AP2IX-9 knockout with CRISPR-CAS9 system.

For disruption of the HXGPRT (TGME49_200320) and AP2IX-9 (TGME49_306620) target genes, we used the multi-guide-RNA (multi-gRNA) CRISPR-Cas9 system as previously published [12]. The CRISPR-Cas9 gRNA plasmid (pSAG1::Cas9-U6::sgUPRT) was provided by David Sibley (Washington University, St. Louis, MO). To generate knockouts in ME49EW Day-2 parasites, three gRNA plasmids were used for the HXGPRT gene and two gRNA plasmids were used for AP2IX-9 gene. To construct knockout plasmids, a common gene replacement plasmid containing a pyrimethamine resistance gene (TgDHFR^{pyr}) was constructed using 3-fragment Gateway protocols (Thermo Fisher Scientific, Waltham, MA). We then PCR amplified a DNA fragment from a plasmid kindly provided by John Boothroyd (Stanford, CA) [35] that encodes a dual expression cassette of tub driven firefly luciferase and gra2 driven GFP. The GFP-Fluc cassette was then inserted into the TgDHFR^{pyr} entry vector using In-Fusion HD cloning (Takara Bio.) that resulted in the triple gene entry plasmid (GFP_Fluc_TgDHFR^{pyr}), which was used for all target gene replacements. To construct specific knockout plasmids, the 5' and 3' untranslated regions (UTRs) of the HXGPRT or AP2IX-9 genes were PCR amplified from Type II parasite genomic DNA (see primer designs below) and the resulting fragments cloned into Gateway entry plasmids. The 5' UTR of each target gene was cloned into the pDONR_P4-P1r vector, and the 3' UTR was cloned into the pDONR_P2r-P3 vector using the BP recombination reaction. After isolation of the pDONR_P4-P1r_5'UTR and pDONR_P2r-P3_3'UTR plasmids for each target gene, they were combined with the GFP_FLuc_TgDHFR^{pyr} plasmid in an LR recombination reaction to generate a final

knockout plasmid for each target gene. The final knockout plasmids were linearized and then combined with the pCrispr/gRNA plasmids before introduction into ME49EW Day2 parasites by nucleofection (see Protocol S1 for full transfection details).

Table of primers used to construct guide RNA plasmids and left and right arm entry vectors for genes TgHXGPRT and AP2IX-9.

Purpose	**primer name**	**Gene**	**Orienta-tion**	**Sequence (5' to 3')**
pCrispr_gRNA	HXGPRT_gRNA1(493)	HXGPRT	Forword	CCACAGAACTTACTTCGGCG GTTTTAGAGCTAGAAATAGC
	HXGPRT_gRNA2(494)	HXGPRT	Forword	ACCAGAACGACAACAGCACA GTTTTAGAGCTAGAAATAGC
	HXGPRT_gRNA3(495)	HXGPRT	Forword	CGTCGAGAAGCGCACAGATC GTTTTAGAGCTAGAAATAGC
pDONR_HX_5'UTR	HX_B4_5'UTR_F(500)	HXGPRT	Forword	GGGG ACA ACT TTG TAT AGA AAA GTT G CTTCCGCGCCGAAAGAAATCTC
	HX_B1r_5'UTR_R(501)	HXGPRT	Reverse	GGGG AC TGC TTT TTT GTA CAA ACT TG GTAACGGACAACACGACCTGGA
pDOON_HX_3'UTR	HX_B2r_3'UTR_F(502)	HXGPRT	Forword	GGGG ACA GCT TTC TTG TAC AAA GTG G ATAGGAGGAAGAAAGACGATCCGTCTG
	HX_B3_3'UTR_R(503)	HXGPRT	Reverse	GGGG AC AAC TTT GTA TAA TAA AGT TG TGCAACTTGTGTAAACGTCAAACTTTCTC
pCrispr_gRNA	AP2IX-9gRNA3	AP2IX-9	Forword	CGACGTCACCAATCAAGCGTGTTTTAGAGCTAGA AATAGC
	AP2IX-9gRNA4	AP2IX-9	Forword	CCTGGCGGGAAAGAAAACTTGTTTTAGAGCTAGA AATAGC
pDONR_AP2IX-9_5'UTR	AP2IX-9_B4_5'UTR_F (287)	AP2IX-9	Forword	GGGG ACA ACT TTG TAT AGA AAA GTT G CATTTTTTAGGTTGAAGAACCGAGCAGC
	AP2IX-9_B1r_5'UTR_R (288)	AP2IX-9	Reverse	GGGG AC TGC TTT TTT GTA CAA ACT TG CAACGGCATGGCCGAACTACG
pDOON_AP2IX-9_3'UTR	AP2IX-9_B2r_3'UTR_F (289)	AP2IX-9	Forword	GGGG ACA GCT TTC TTG TAC AAA GTG G GTTAACGTGAGTTGCGCAGTCTTGC
	AP2IX-9_B3_3'UTR_R (290)	AP2IX-9	Reverse	GGGG AC AAC TTT GTA TAA TAA AGT TG CCCGCTGGAAAAAAGAAAGCGAC

Other protocols in supplement.

Protocol S1: Cyst and bradyzoite purification

Protocol S2: Producing transgenic cysts

Protocol S3: Cloning transgenic tissue cysts.

Protocol S4: Freezing cysts in brain homogenates.

References

1. Sullivan, W.J., Jr. and V. Jeffers, *Mechanisms of Toxoplasma gondii persistence and latency.* FEMS Microbiol Rev, 2012. **36**(3): p. 717-33.
2. Goerner, A.L., et al., *An ex vivo model of Toxoplasma recrudescence.* Biorxiv 2020/101931 [Preprint], , 2020. **Available from:https://doi.org/10.1101/2020.05.18.101931**
3. Boillat, M., et al., *Neuroinflammation-Associated Aspecific Manipulation of Mouse Predator Fear by Toxoplasma gondii.* Cell Rep, 2020. **30**(2): p. 320-334 e6.
4. Schluter, D. and A. Barragan, *Advances and Challenges in Understanding Cerebral Toxoplasmosis.* Front Immunol, 2019. **10**: p. 242.
5. Cabral, C.M., et al., *Neurons are the Primary Target Cell for the Brain-Tropic Intracellular Parasite Toxoplasma gondii.* PLoS Pathog, 2016. **12**(2): p. e1005447.
6. Song, H.B., et al., *Investigation of tissue cysts in the retina in a mouse model of ocular toxoplasmosis: distribution and interaction with glial cells.* Parasitol Res, 2018. **117**(8): p. 2597-2605.
7. Ndubuizu, O. and J.C. LaManna, *Brain tissue oxygen concentration measurements.* Antioxid Redox Signal, 2007. **9**(8): p. 1207-19.
8. Su, C., et al., *Identification of quantitative trait loci controlling acute virulence in Toxoplasma gondii.* Proc Natl Acad Sci U S A, 2002. **99**(16): p. 10753-8.
9. Donald, R.G. and D.S. Roos, *Stable molecular transformation of Toxoplasma gondii: a selectable dihydrofolate reductase-thymidylate synthase marker based on drug-resistance mutations in malaria.* Proc Natl Acad Sci U S A, 1993. **90**(24): p. 11703-7.
10. Lemgruber, L., et al., *The organization of the wall filaments and characterization of the matrix structures of Toxoplasma gondii cyst form.* Cell Microbiol, 2011. **13**(12): p. 1920-32.
11. Altschul, S.F., et al., *The construction and use of log-odds substitution scores for multiple sequence alignment.* PLoS Comput Biol, 2010. **6**(7): p. e1000852.
12. Hong, D.P., J.B. Radke, and M.W. White, *Opposing Transcriptional Mechanisms Regulate Toxoplasma Development.* mSphere, 2017. **2**(1).
13. Radke, J.B., et al., *ApiAP2 transcription factor restricts development of the Toxoplasma tissue cyst.* Proc Natl Acad Sci U S A, 2013. **110**(17): p. 6871-6.
14. Radke, J.B., et al., *Transcriptional repression by ApiAP2 factors is central to chronic toxoplasmosis.* PLoS Pathog, 2018. **14**(5): p. e1007035.
15. Kim, K., D. Soldati, and J.C. Boothroyd, *Gene replacement in Toxoplasma gondii with chloramphenicol acetyltransferase as selectable marker.* Science, 1993. **262**(5135): p. 911-4.
16. Soldati, D. and J.C. Boothroyd, *Transient transfection and expression in the obligate intracellular parasite Toxoplasma gondii.* Science, 1993. **260**(5106): p. 349-52.
17. Donald, R.G., et al., *Insertional tagging, cloning, and expression of the Toxoplasma gondii hypoxanthine-xanthine-guanine phosphoribosyltransferase gene. Use as a selectable marker for stable transformation.* J Biol Chem, 1996. **271**(24): p. 14010-9.
18. Messina, M., et al., *Stable DNA transformation of Toxoplasma gondii using phleomycin selection.* Gene, 1995. **165**(2): p. 213-7.
19. Behnke, M.S., A. Khan, and L.D. Sibley, *Genetic mapping reveals that sinefungin resistance in Toxoplasma gondii is controlled by a putative amino acid transporter locus that can be used as a negative selectable marker.* Eukaryot Cell, 2015. **14**(2): p. 140-8.
20. Huynh, M.H. and V.B. Carruthers, *Tagging of endogenous genes in a Toxoplasma gondii strain lacking Ku80.* Eukaryot Cell, 2009. **8**(4): p. 530-9.
21. Fox, B.A., et al., *Efficient gene replacements in Toxoplasma gondii strains deficient for nonhomologous end joining.* Eukaryot Cell, 2009. **8**(4): p. 520-9.
22. Winiger, R.R. and A.B. Hehl, *A streamlined CRISPR/Cas9 approach for fast genome editing in Toxoplasma gondii and Besnoitia besnoiti.* J Biol Methods, 2020. **7**(4): p. e140.
23. Sharifpour, M.F., et al., *A GRA2 minimal promoter improves the efficiency of TATi / Tet-Off conditional regulation of gene expression in Toxoplasma gondii.* Mol Biochem Parasitol, 2021. **244**: p. 111384.
24. Brown, K.M., S. Long, and L.D. Sibley, *Plasma Membrane Association by N-Acylation Governs PKG Function in Toxoplasma gondii.* mBio, 2017. **8**(3).

25. Wang, Y., et al., *Genome-wide screens identify Toxoplasma gondii determinants of parasite fitness in IFNgamma-activated murine macrophages.* Nat Commun, 2020. **11**(1): p. 5258.
26. Donald, R.G. and D.S. Roos, *Gene knock-outs and allelic replacements in Toxoplasma gondii: HXGPRT as a selectable marker for hit-and-run mutagenesis.* Mol Biochem Parasitol, 1998. **91**(2): p. 295-305.
27. Roos, D.S., et al., *Tagging genes and trapping promoters in Toxoplasma gondii by insertional mutagenesis.* Methods, 1997. **13**(2): p. 112-22.
28. Saraf, P., et al., *On the determination of Toxoplasma gondii virulence in mice.* Exp Parasitol, 2017. **174**: p. 25-30.
29. Jeffers, V., et al., *A latent ability to persist: differentiation in Toxoplasma gondii.* Cell Mol Life Sci, 2018. **75**(13): p. 2355-2373.
30. Jerome, M.E., et al., *Toxoplasma gondii bradyzoites form spontaneously during sporozoite-initiated development.* Infect Immun, 1998. **66**(10): p. 4838-44.
31. Radke, J.R., et al., *The transcriptome of Toxoplasma gondii.* BMC Biol, 2005. **3**: p. 26.
32. Waldman, B.S., et al., *Identification of a Master Regulator of Differentiation in Toxoplasma.* Cell, 2020. **180**(2): p. 359-372 e16.
33. Roos, D.S., et al., *Molecular tools for genetic dissection of the protozoan parasite Toxoplasma gondii.* Methods Cell Biol, 1994. **45**: p. 27-63.
34. Dubey, J.P., *Mouse pathogenicity of Toxoplasma gondii isolated from a goat.* Am J Vet Res, 1980. **41**(3): p. 427-9.
35. Kim, S.K., A. Karasov, and J.C. Boothroyd, *Bradyzoite-specific surface antigen SRS9 plays a role in maintaining Toxoplasma gondii persistence in the brain and in host control of parasite replication in the intestine.* Infect Immun, 2007. **75**(4): p. 1626-34.

Engineering *Toxoplasma gondii* transgenic tissue cysts.
Figures and legends

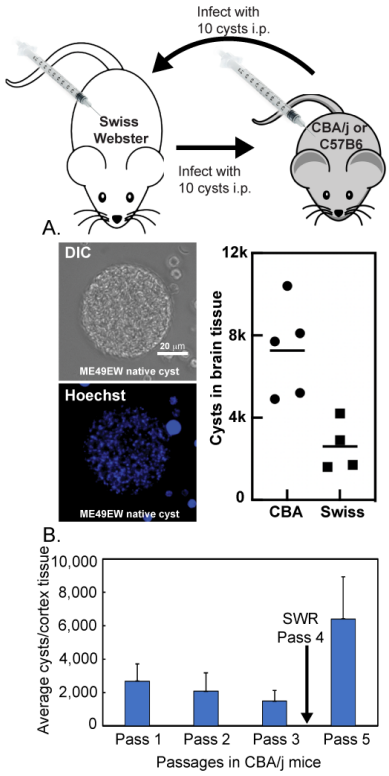

Figure 1. Alternating mouse strain infections stabilizes tissue cyst yields in brain cortex tissue.

The ME49EW strain is maintained in the relatively resistant Swiss Webster (SWR/j) mouse strain by a 10 cyst inoculation (i.p.) every 30-60 days. Tissue cysts from SWR/j brain homogenates are used to amplify tissue cysts numbers in the sensitive CBA/j mouse strain (10 cyst/mouse, 30-50 d.p.i.). **[A.]** Representative example of a ME49EW brain tissue cyst purified from mouse brain cortex tissue at 40 d.p.i. Brain tissue cyst numbers (cortex only) are higher in CBA/j versus SWR/j mice. **[B.]** Sequential passage in CBA/j mice can result in a progressive decline in tissue cyst number after multiple passages. If the single mouse strain passages are not excessive, a single passage through SWR/j mice can restore higher cyst numbers in the next CBA/j infection. Average cyst numbers for each CBA/j passage involved >5 mice/passage.

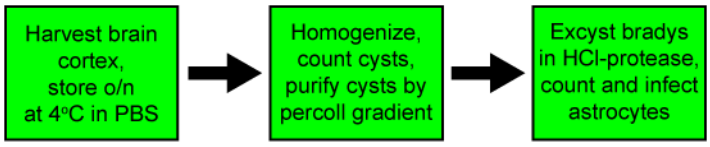

Me49EW parasite yields				
Harvest Date	**Days PI**	**# mice**	**Bradyzoite yield (10^6)**	**Bradys/ mouse (10^6)**
7/8/19	40	20	22.0	1.1
1/7/20	41	22	31.3	1.4
7/7/20	41	20	11.9	0.6
8/18/20	48	20	29.6	1.5
12/16/20	47	20	15.7	0.8
3/4/21	42	20	25.7	1.3
11/15/21	41	15	48.6	3.2
8/12/21	44	25	36.1	1.4
8/26/21	43	11	15.5	1.4
9/9/21	44	15	24.2	1.6
11/1/21	42	22	27.6	1.3
		210 total	288.2 total	1.4 average

Figure 2. Producing ME49EW tissue cysts and bradyzoites is robust and reproducible.
Key steps in purifying ME49EW tissue cysts and excysting bradyzoites are indicated. An average of 1.4 million purified bradyzoites are obtained from each CBA/j mouse at 40 d.p.i. (10 cysts i.p.), which is consistent year over year. Detailed procedures for purifying cysts and bradyzoites are included in Protocol S1.

A. Growth in low oxygen (5%)				
Day Inf./ Harvested	**Input (10^6)**	**Output (10^6)**	**Total fold**	**Fold per day**
D0/D3	1.5	24.4	16.29	5.43
D3/D5	1.5	7.42	4.95	2.47
D5/D7	1.5	1.95	1.3	0.65
Growth in high oxygen (21%)				
Day Inf./ Harvested	**Input (10^6)**	**Output (10^6)**	**Total fold**	**Fold per day**
D0/D3	1.5	28	18.67	6.22
D3/D5	1.5	3.08	2.05	1.03
D5/D7	1.5	0.54	0.36	0.18
Production of Day-2 fast-tachyzoites				
Harvest Date	**Days PI**	**Brady inf (10^6)**	**Day-2 yield (10^6)**	**Fold amplification**
10/5/21	40	10	56.4	5.6
10/25/21	47	15	59	3.9

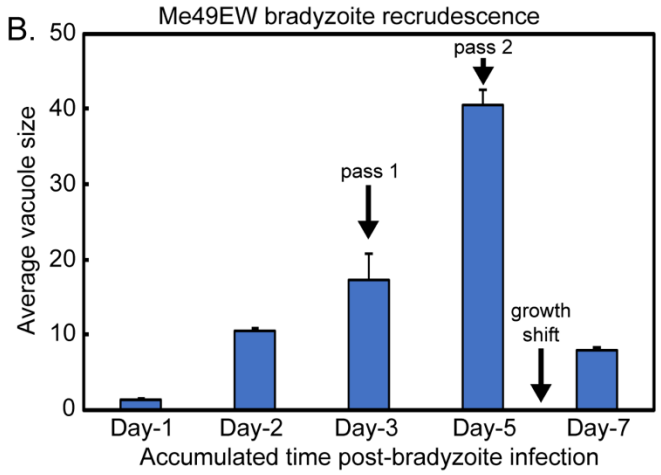

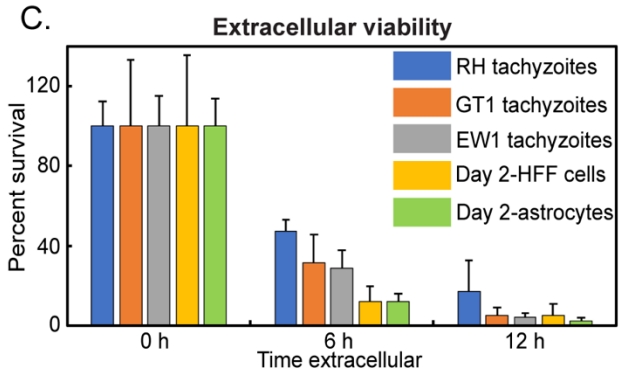

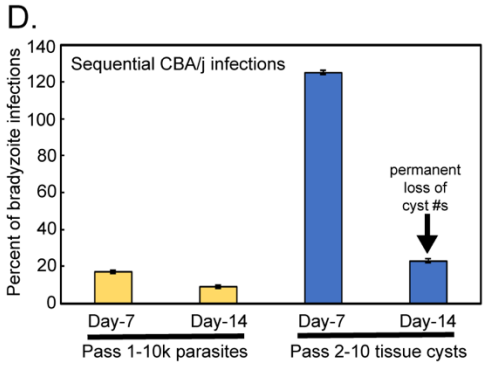

Figure 3. Critical features of the ex vivo recrudescence assay.
[A. and B.] ME49EW bradyzoite recrudescence infections in primary mouse astrocytes are influenced by oxygen gas concentrations. Table:Parasite population growth is improved by lowering the oxygen levels to 5% as compared to standard atmospheric oxygen (21%) conditions in astrocyte cultures (D3/D5 and D5/D7) beyond the first astrocyte monolayer infected with excysted-bradyzoites (D0/D3). Note parasite replication in the first 24 h of bradyzoite-infected cultures is minimal (~1.4 fold at D1). Relevant to nucleofection experiments, a 4-5 fold amplification of parasite numbers in Day-2 populations as compared to bradyzoite inoculations at Day-0 was reproducible (bradyzoites were obtained from mice ≥40 days post-infection). Graph:Average vacuole size was determined in the first astrocyte monolayer at Days 1-3, in the second monolayer at Day-5, and in the third monolayer at Day-7. All times indicated are accumulative with respect to the excysted-bradyzoite infection at Day-0. A reproducible shift to significantly slower parasite growth occurs beyond Day-5 in these cultures. **[C.]** Extracellular stability of Day 2-recrudescence parasites from ME49EW bradyzoite infections of HFF or astrocyte monolayers compared to lab-adapted strains, Type II-ME49EW1 or Type I-RH and -GT1 strain tachyzoites (see Material and Methods for experimental details) All results are compared to time-zero. Note that the ME49EW1 strain is more stable in media than the ME49EW Day-2 parent, which is likely the result of cell culture adaptation. **[D.]** Infections of CBA/j mice with Day-7 or Day-14 parasite populations grown in astrocytes produce fewer brain cysts (gold bars) as compared to excysted-bradyzoite infections. First round of CBA/j infections (Pass 1)=10,000 parasites i.p. A second round of CBA/j infections (Pass 2, 10 cysts i.p) using tissue cysts from Pass 1 mice (blue bars) is shown. Average brain cortex tissue cyst numbers were determined from groups of five CBA/j mice at 30 d.p.i.

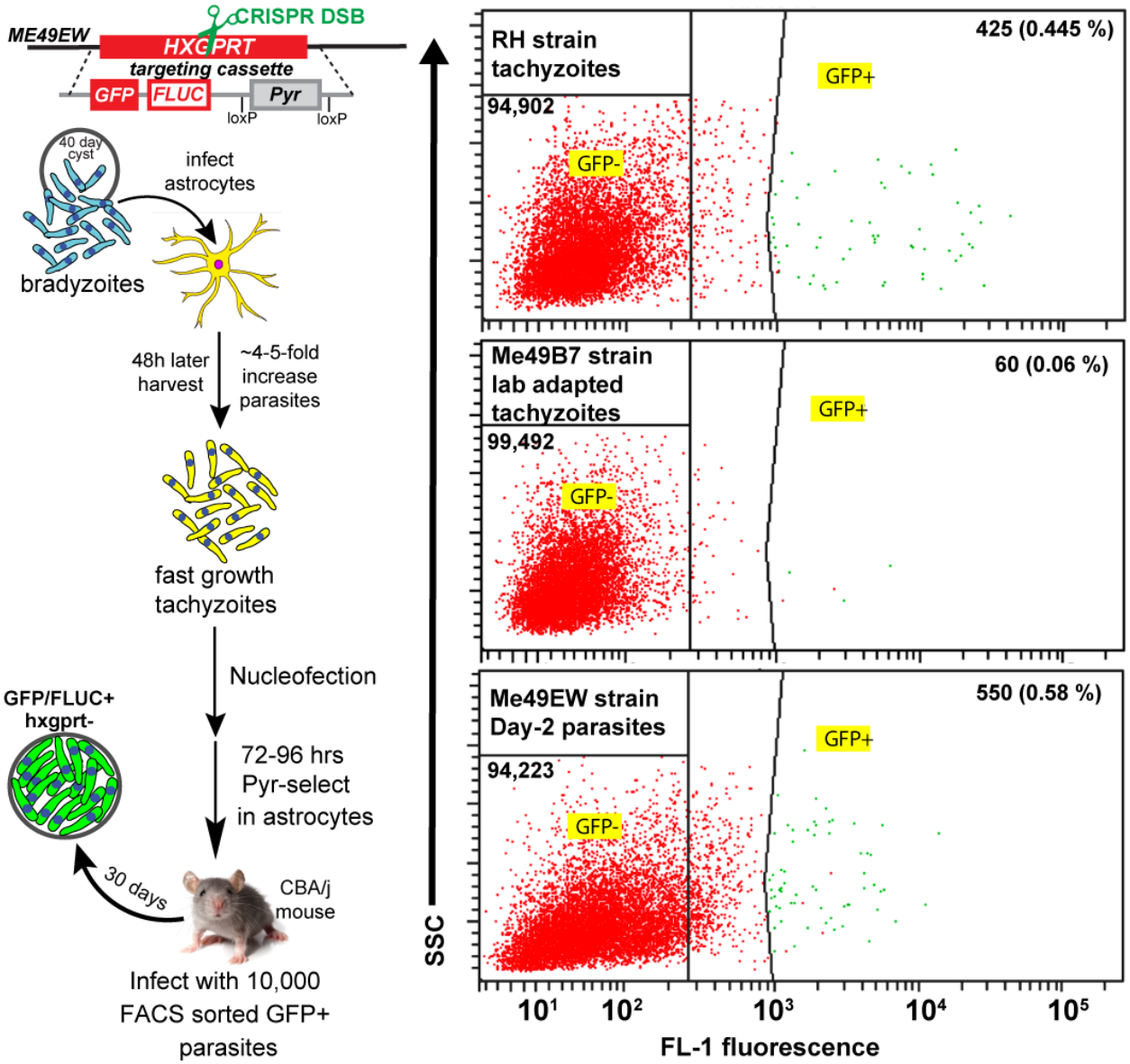

Figure 4. Me49EW Day-2 parasites are transformed with equal efficiency as the RH strain.
Cartoon: Overview of the protocol for generating transgenic tissue cysts in mice. For complete details see Protocol S2.
Dot plots: The TgHXGPRT gene was targeted for CRISPR-assisted knockout in two laboratory strains (RH and ME49B7) and ME49EW Day-2 recrudescent parasites. Following nucleofection and 96 h post-pyrimethamine (0.5μM) selection in astrocytes, parasites were purified and 100,000 live events/strain analyzed by flow cytometry. Gates defining GFP- versus GFP+ parasites are shown for each strain transfected.

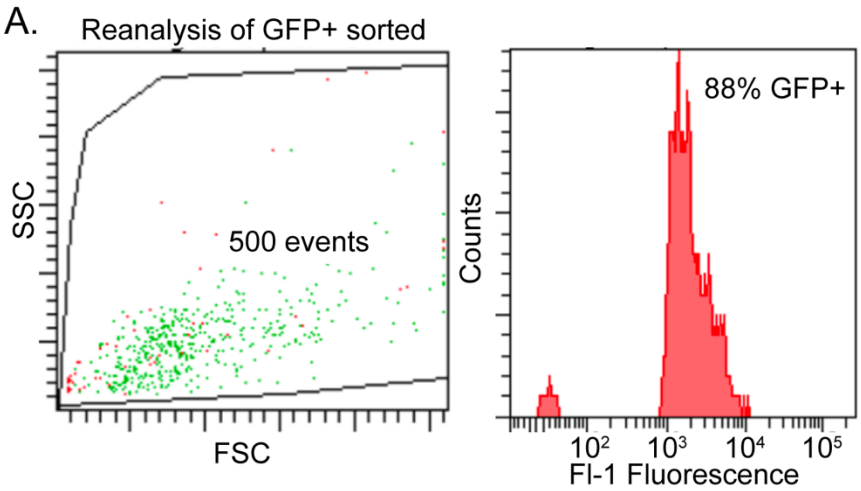

B. Tissue cyst numbers 30day PI

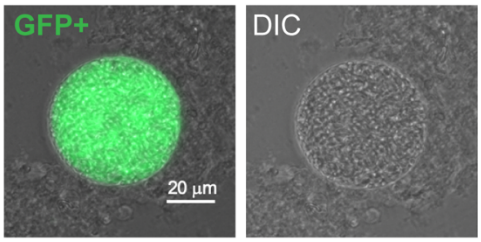

brain cortex	total cysts	% GFP+
1	2500	64
2	1666	72
3	2500	56
4	2083	64
5	2900	52

Figure 5. GFP+ sorted populations are infectious and produce GFP+ tissue cysts in mice.
[A.] GFP+ parasites from the ME49EW Day-2 nucleofected population in Fig. 4 were FACS sorted (55,000 total sort). The sorted parasites reanalyzed by FACS (Dot Plot) were 88% GFP+ (histogram) representing a 150 fold enrichment over the pre-sort population (Fig. 4. Day-2 parasites 0.58% GFP+). **[B.]** GFP+ sorted parasites were used to infect five CBA/j mice (10,000 parasites i.p./mouse). At 30 d.p.i., brain cortex tissue was harvested and total tissue cysts and GFP+ expression determined. A representative image of GFP+ transgenic tissue cyst is shown (live GFP fluorescence compared to DIC image, 1000x).

A.

TL Cysts Counted	GFP Pos	GFP Neg
74	94.6%	5.4%
58	94.8%	5.2%
54	74.1%	25.9%
50	94%	6%
50	100%	0%
56	83.9%	16.1%
60	0%	100%
50	70%	30%
50	100%	0%
50	0%	100%
50	100%	0%
60	100%	0%
116	94%	6%
50	38%	62%
70	34.3%	65.7%
50	86%	14%
58	100%	0%
72	6.9%	93.1%
50	0%	100%

B.

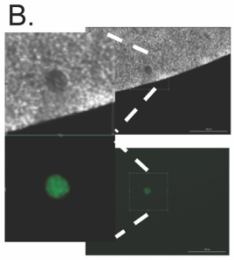

Brain homogenate

mouse #	TOTAL
1	400
2	1100
3	1500
4	1300

Percoll purified

mouse #	TOTAL
1	2200
2	900
3	1100
4	1800
5	700

C.

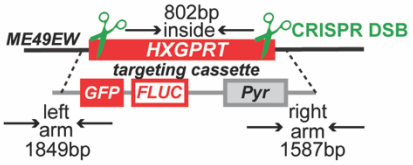

D. Clonal tissue cyst screening 30day PI

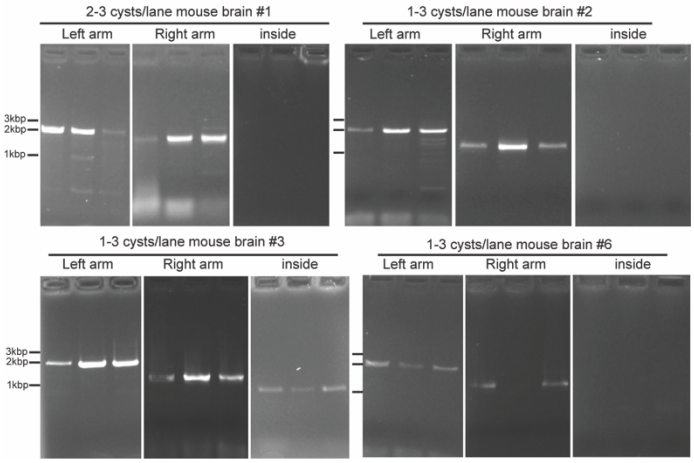

Figure 6. Cloning gene knockout transgenic cysts.
[A.] GFP+ tissue cysts were mixed 1:1 with GFP- tissue cysts (ME49EW strains) and diluted to 10 cysts/ml of PBS. Twenty CBA/j mice were infected i.p with 2 cysts/mouse (one mouse died before cyst analysis). At 30 d.p.i., cortex brain tissue was harvested from each mouse and tissue cysts purified by percoll gradient (Protocol S1). A minimum of 50 live tissue cysts from each mouse were evaluated for GFP+ expression by fluorescence microscopy. **[B.]** Single tissue cysts are infectious and produce substantial tissue cyst numbers in CBA/j mice. Single GFP+ tissue cysts from brain homogenates or following percoll gradient purification were isolated by limiting dilution in 96 well optical plates. At 30 d.p.i., tissue cyst counts in brain homogenates from the nine infected mice indicated were determined. Note, no GFP-negative tissue cysts were observed in mice infected with a single GFP+ cysts (all 100% GFP+). **[C.]** Overview of AP2IX-9 knockout strategy and PCR screening strategy. The TgHXGPRT coding region was replaced by a three gene cassette of GFP, firefly luciferase, and pyrimethamine-resistant DHFR [9]. **[D.]** PCR analysis of the knockout of the TgHXGPRT gene in ME49EW tissue cysts was confirmed in single cyst infections of mice. The presence of the correct left and right arm DNA fragments in ME49EW::*Δhxgprt* parasite gDNA verified the correct double cross-over had occurred in the clone (left/right arm gels). The failure to amplify a TgHXGPRT 802bp internal gDNA coding fragment (inside gels) indicated a clean TgHXGPRT knockout.

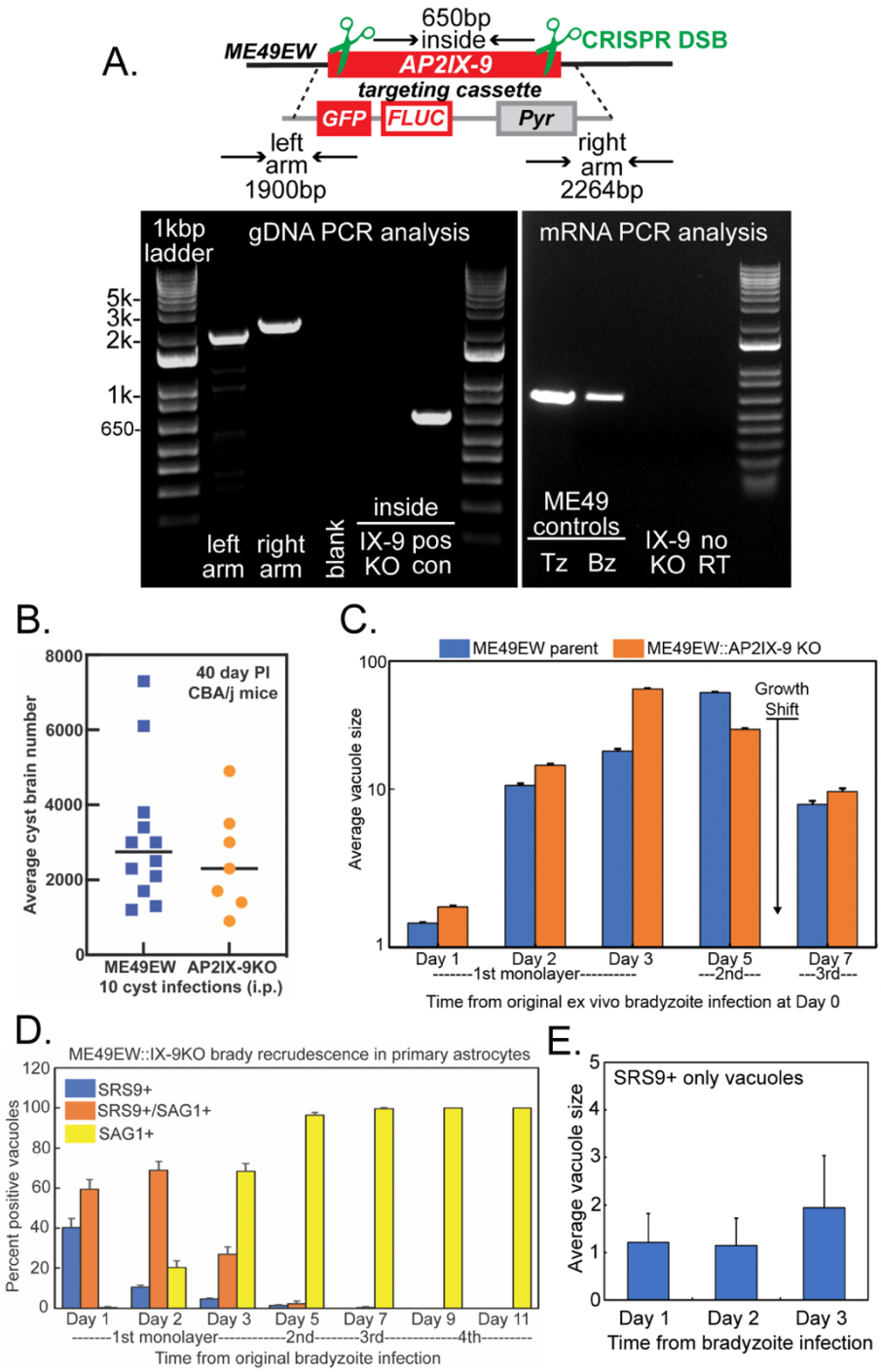

Figure 7. AP2IX-9 is required for bradyzoite to bradyzoite recrudescence.
[A.] Cartoon: Overview of AP2IX-9 knockout strategy. PCR analysis: Knockout (KO) of the AP2IX-9 gene in ME49EW tissue cysts was confirmed in a GFP+-tissue cyst cloned by single cyst mouse infection and then expanded in CBA/j mice. The presence of the correct left and right arm DNA fragments in ME49EW::*Δap2IX-9* parasite gDNA verified the correct double cross-over had occurred in the clone (left gel). The failure to amplify a AP2IX-9 650bp internal gDNA coding fragment as well as the absence of AP2IX-9 mRNA (right gel) was further evidence of the AP2IX-9 gene knockout. RNA purified from ME49EW tachyzoites and cysts provided positive controls for AP2IX-9 mRNA expression. The no reverse transcriptase control (no RT) was included to verify the ME49EW::*Δap2IX-9* RNA sample was free of contaminating gDNA. **[B]**. Tissue cyst counts for the ME49EW::*Δap2IX-9* strain compared to the ME49EW parent strain. **[C.].** Purified ME49EW::*Δap2IX-9* bradyzoites initiate the identical growth transitions (fast growth followed by switch to slow growth) in murine astrocytes as the parent ME49EW strain [2]. **[D.]** The timing of SRS9 and SAG1 surface antigen expression during ME49EW::*Δap2IX-9* bradyzoite recrudescence was quantified in four sequentially infected astrocyte monolayers. **[E].** Average vacuole size of SRS9+ only vacuoles during Day 1-3 ME49EW::*Δap2IX-9* bradyzoite recrudescence.